Sighting of El Chichón Sulfur Dioxide Clouds with the Nimbus 7 Total Ozone Mapping Spectrometer

Abstract. *The eruptions of El Chichón volcano on 28 March and 3 and 4 April 1982 were observed by the Nimbus 7 total ozone mapping spectrometer due to strong absorption by volcanic gases at the shortest wavelengths of the spectrometer (312.5 and 317.5 nanometers). These ultraviolet pictures permit a measurement of the volume, dispersion, and drift of volcanic gas clouds. The tropospheric clouds were rapidly dispersed in westerly winds while persistent stratospheric clouds drifted in easterly winds at speeds up to 13 meters per second. The spectral reflectance is consistent with sulfur dioxide absorption and rules out carbon disulfide as a major constituent. A preliminary estimate of the mass of sulfur dioxide deposited in the stratosphere by the large eruptions on 3 and 4 April is 3.3 × 10^6 tons. Prior estimates of volcanic cloud volume were based on extrapolation of locally measured sulfur dioxide concentrations.*

The major eruptions of El Chichón volcano in southern Mexico (17.3°N, 95.2°W) were observed with the total ozone mapping spectrometer (TOMS) instrument on the Nimbus 7 satellite. The eruptions began on 28 March 1982, recurred on 3 April, and culminated in the largest eruption on 4 April 1982 (*1*). The volcanic clouds caused strong absorption in the shortest wavelength channels of the TOMS instrument, which was designed to map the daily, global total ozone field with high spatial resolution by measuring the ultraviolet albedo of the atmosphere.

Volcanic gases are transparent to visible radiation and their infrared bands are generally masked or confounded by the permanent atmospheric constituents (CO_2, H_2O, and O_3). Thus the volcanic clouds appearing in published satellite images are composed of ash and aerosols. The gaseous emissions have been sampled from high-altitude aircraft and the total gas volume is derived indirectly from these point measurements and estimates of flow rates of plume material. The ability of TOMS to resolve the full cloud permits a measurement of the volume of the gaseous cloud elements that absorb at near-ultraviolet wavelengths.

The TOMS instrument (*2*) is an Ebert monochromator with serially sampled, fixed exit slits set at 312.5, 317.5, 331.2, 339.8, 360.0, and 380.0 nm, with a fixed spectral band pass of 1.0 nm. The 3° by 3° field of view is stepped to 35 cross-track positions each 8 seconds as the spacecraft moves in a sun-synchronous noon-midnight polar orbit. This design produces complete contiguous sampling of the atmospheric radiance in 2800-km-wide swaths centered on the orbit paths. The spatial resolution at the nadir is 50 by 50 km and increases to 150 by 300 km at the far scan positions.

Total column ozone is determined by comparing observed with theoretical albedos, which were computed with an absorbing, multiple Rayleigh scattering radiative transfer model for the full range of observing and geophysical conditions (*2*). The resulting ozone data are comparable to those from Dobson spectrophotometer stations.

The TOMS atmospheric model fails when large amounts of absorbing gases other than ozone are present. These deviations can be detected under certain conditions and are the basis for the present volcanic cloud observations. The contaminated atmospheric volumes are found to produce lower albedos at 312.5 and 317.5 nm and much higher apparent total ozone amounts in the volcanic cloud area than in the surroundings. This allows us to determine the location and morphology of the clouds in tropical regions, where the spatial variance of total ozone is small.

Each of the major El Chichón eruptions produced clouds which were discernible as anomalies in the daily TOMS ozone maps. The initial eruption at 0532 GMT on 29 March 1982 (local time = GMT − 6 hours) was first viewed at 1816 GMT. An arc-shaped cloud covered an area extending east from the volcano across the Yucatan Peninsula and west to 102°W, 16°N (a length of 1400 km). The zonal spreading of the cloud is due to shearing of the initially vertical column by tropospheric westerly and stratospheric easterly winds, as observed in radiosonde ascents from Mexico and Hawaii.

The major eruption on 4 April and residual clouds from the lesser eruptions on 3 April were observed at local noon on 4 April as a cloud mass of high optical depth with a sinuous trail of material extending across Cuba. The appearance of this cloud on 5 April as an elongated patch of higher apparent ozone amounts (brown and yellow colors) across southern Mexico is shown in the lower half of the cover photograph. The stratospheric cloud extends over the Pacific Ocean to 112°W, while the tropospheric cloud, fed by fallout from the stratosphere, has drifted across Jamaica and Haiti.

Cloud drift speeds are obtained from outlines of the clouds on 5, 6, and 7 April as shown in Fig. 1. The leading edge of the stratospheric cloud moves about 11° in longitude per day (13 m/sec) to the west. Drift estimates from the cloud boundary could be in error if the absorbing material is photolyzed or chemically converted to other species. Therefore, the positions of the centroids of the major lobe (A) and the secondary lobe (B) were estimated on each day (see Fig. 1). These positions show the same average displacement as the leading edge of the cloud, indicating that the loss rate of the absorbing species is relatively small.

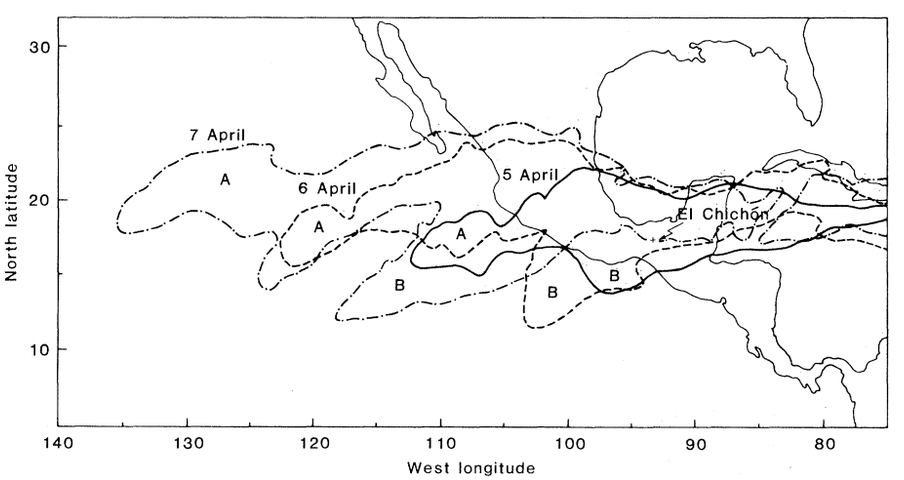

Fig. 1. Outlines of the SO_2 cloud produced by the major eruption of El Chichón on 4 April 1982. The cloud boundaries are shown for 5, 6, and 7 April. The stratospheric cloud drifts to the west and north from the volcano. Cloud velocity was estimated from the motion of lobes A and B and from the leading edge of lobe A.

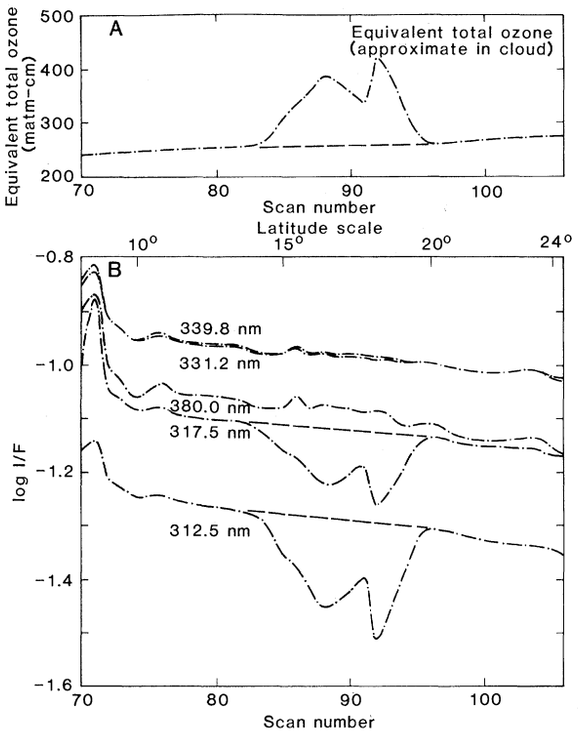

Fig. 2. Effects of the El Chichón cloud on TOMS radiances and total ozone retrievals. (A) Equivalent total ozone along a trace across the western end of the 5 April cloud. (B) Logarithm of spectral reflectivity along the same trace for five TOMS wavelengths, showing cloud absorption at the two shortest wavelengths.

The apparent ozone perturbation by the volcanic cloud is shown in Fig. 2A. This south-to-north trace across major lobe A of the 5 April cloud was obtained by selecting data from the TOMS view angle of 9° left of the nadir for a series of 35 sequential scans between 8° and 24° N. The cloud appears as a large perturbation above the normal tropical total ozone, which increases from 250 matm-cm at 10°N to 280 matm-cm at 24°N (1 matm-cm = 2.687×10^{16} molecules per square centimeter). The cloud absorption is equivalent to total ozone amounts greater than 400 matm-cm, based on extrapolation of the albedo–total ozone relation.

The spectral characteristics of the cloud can be deduced from the spectral reflectance at the TOMS wavelengths. Figure 2B shows the logarithm of the reflectance (earth radiance, I, divided by solar irradiance, F) for the same cloud trace as Fig. 2A. A large decrease in reflectance due to absorption is found at 312.5 and 317.5 nm but not at longer wavelengths. These effects can be compared with that of a cumulus cloud mass which appears at scan number 71 as a reflectance maximum, common to all wavelengths, which does not perturb the total ozone retrieval. Volcanic ash with a flat spectral reflectivity has a similar, but much smaller, effect on the radiances.

The wavelength dependence of the cloud absorption allows discrimination of the two known volcanic constituents (*3*) that absorb at TOMS wavelength. These are SO_2, with an absorption band between 260 and 320 nm, and CS_2, which absorbs between 300 and 330 nm (*3*). Carbon disulfide (and ozone) would produce clearly perceptible absorption at 331.2 and 339.8 nm but SO_2 would not. Since no absorption appears at these wavelengths we conclude that SO_2 is the major gaseous constituent.

The presence of SO_2 can be further tested by comparison of column amounts at the two absorbed wavelengths. We assume that the SO_2 is isolated from the primary Rayleigh scattering volumes in the troposphere and that the stratospheric ozone is not perturbed. The relative reflectance over the cloud at wavelength λ, total ozone amount Ω, and column SO_2 amount S is given by

$$\log \frac{I'(\lambda,\Omega,S)}{F(\lambda)} = \log \frac{I(\lambda,\Omega,0)}{F(\lambda)} - \alpha_{SO_2}(\lambda) S \mu \quad (1)$$

where $I(\lambda,\Omega,0)$ is the unperturbed radiance, $F(\lambda)$ is the incident solar irradiance, α_{SO_2} is the SO_2 absorption coefficient (*3*), and μ is the slant path length through the SO_2 layer. Vertical column SO_2 is then calculated from

$$S = \frac{-\log I'/I}{\alpha_{SO_2}\mu} \quad (2)$$

In practice, the ratio of radiances for pairs of TOMS wavelengths is used to decrease the sensitivity to errors in external parameters including air pressure and reflectivity at the lower boundary.

The background radiance is estimated by interpolation between the unperturbed regions on either side of the cloud, as shown by the dashed lines on the 312.5- and 317.5-nm curves in Fig. 2B. The column SO_2 amount observed at the largest perturbation (scan number 92) is 61 matm-cm with the wavelength pair 312.5 and 331.2 nm and 67 matm-cm with the wavelength pair 317.5 and 339.8 nm. The 10 percent difference is believed to be within the measurement errors of SO_2 absorption coefficients and their temperature dependence. Available measurements are at room temperature, whereas the temperature of the stratospheric SO_2 cloud was below −50°C. The results are therefore consistent with SO_2 absorption although the column amounts are tentative. A definitive analysis will require data on cross sections at low temperatures and an accounting for aerosol effects and ozone changes in the cloud. A preliminary summation of the total SO_2 content of the stratospheric cloud on 6 April is 3.3 $(+1.0, -0.2) \times 10^6$ tons, based on the average SO_2 column amount of 42 matm-cm and a cloud area of 2.8×10^6 km^2. Conventional estimates from aircraft sampling are not available due to the 26-km altitude of the cloud found by LIDAR at Mauna Loa (*4*). Additional sulfur, present as H_2S, would not be detected by TOMS.

Volcanic SO_2 has been considered to be the principal precursor of stratospheric H_2SO_4 aerosols, which have been implicated in global cooling observed after past major eruptions. Estimates of the total amount of SO_2 based on point samples of the clouds are highly variable due to uncertainties in both average concentration and total gas cloud volume. The TOMS observations are shown here to be useful for determining column SO_2 amounts throughout a dispersing volcanic cloud. From this the total amount of SO_2 injected into the stratosphere is determined. The rate of change of the SO_2 volume obtained from the series of TOMS maps then can be used to verify models of the chemical conversion of SO_2 to H_2SO_4. These measurements are expected to lead to better estimates of volcanic source strengths and to a better understanding of sulfur chemistry in the stratosphere.

ARLIN J. KRUEGER
NASA/Goddard Space Flight Center, Greenbelt, Maryland 20771

References and Notes

1. Smithsonian Institution, *SEAN (Sci. Event Alert Network) Bull.* **7**, 3 (1982).
2. D. F. Heath, A. J. Krueger, H. A. Roeder, B. D. Henderson, *Opt. Eng.* **14**, 323 (1975); A. J. Fleig, K. F. Klenk, P. K. Bhartia, D. Gordon, *NASA Ref. Publ. RP 1096* (1982).
3. Possible cloud constituents were considered to be SO_2, CS_2, COS, H_2S, H_2SO_4, HCl, HF, HBr, H_2, CO, and CO_2. All except SO_2 and CS_2 are transparent at TOMS wavelengths [H. Okabe, *Photochemistry of Small Molecules* (Wiley, New York, 1978)]. The SO_2 cross sections were obtained by C. Y. R. Wu and D. L. Judge [*Geophys. Res. Lett.* **8**, 769 (1981); unpublished data]. These cross sections are in agreement with measurements by M. M. Millan and R. M. Hoff (Atmospheric Environment Service, Downsview, Ontario) at 312.5 nm, but are 25 percent higher at 317.5 nm. Cross-section data on CS_2 were obtained from P. H. Wine, W. L. Chameides, and A. R. Ravishankara [*Geophys. Res. Lett.* **8**, 543 (1981); unpublished data].
4. K. L. Coulson, T. E. Defoor, J. Deluisi, *Eos* **63**, 897 (Abstr.) (1982).

5. I thank the Landsat/Nimbus Project Office and the General Electric, Bendix, and Systems and Applied Sciences Companies for their assistance in providing real-time processing of TOMS data. J. A. Gatlin provided the color TOMS images. Funding for real-time processing of North American TOMS orbits was provided by the NASA Office of Aerospace Technology.

17 September 1982; revised 13 December 1982

Venus: Global Surface Radio Emissivity

Abstract. *Observations of thermal radio emission from the surface of Venus, made by the Pioneer Venus radar mapper at a wavelength of 17 centimeters, show variations that are dominated by changes in surface emissivity. The regions of lowest emissivity (0.54 ± 0.05 for the highland areas of Aphrodite Terra and Theia Mons) correspond closely to regions of high radar reflectivity reported earlier. These results support the inference of inclusions of material with high electrical conductivity in the surface rock of these areas.*

As part of its normal operating sequence, the Pioneer Venus radar mapper experiment (*1*) measured the background radio noise reaching the radar receiver at a wavelength of 17 cm. Its radar antenna, fixed to the spinning spacecraft, made two such background measurements each 12-second rotation, one while the antenna was pointing down to the hot planet (the planet calibration) and the other while the antenna was pointing outward to cold space (the space calibration). During a typical daily orbital pass, over 300 pairs of such radiometric measurements were made, their primary use being to monitor receiver performance, which proved to be extremely stable. Because of the inclined orbit, coverage was restricted to planetary latitudes between 75°N and 75°S. Nonetheless, because the planet rotated under the orbital plane during the experiment's 28-month lifetime, 94 percent of the planetary surface was observed.

The antenna "footprint," the area of planetary surface filling the beam during a planet calibration measurement, was determined by the antenna's 30° acceptance cone angle, being 90 km in diameter at the lowest periapsis altitude of 150 km and increasing nearly linearly with altitude as the spacecraft climbed to the maximum radar operating limit of 4700 km. This variation is in contrast with that of the radar altimeter's footprint, which was largely controlled by the radar waveform, rising from 7 by 23 km at 200-km altitude near periapsis to about 100-km diameter at 4000-km altitude (*2*).

The global map of the planet calibration data is shown in Fig. 1, where the featureless background has a brightness temperature of about 635 K (*3*). Areas darker than their surroundings denote a reduction in received thermal flux; the gradual darkening below 50°S results from an increasing angular offset of the antenna from nadir during the planet calibration in that region, caused by an antenna steering limitation (*1*), whereas localized dark regions are associated with reduced thermal emission from the surface. These latter areas have brightness temperatures ranging down to 405 K and correspond closely with elevated regions located by the radar altimeter (*2*). The areas of reduced emission are associated with Theia Mons at 282°E, 23°N; Maxwell Mons at 5°E, 63°N; Aphrodite Terra at 95°E, 5°S and at 125°E, 10°S; and Ozza Mons at 200°E, 2°N. The diameter of the footprint at Theia Mons is 95 km, at Maxwell Mons is 1100 km, and varies from 110 to 130 km for the remaining features.

The physical surface temperature of the median plains, which lie within 1 km of the median planetary radius of 6051.6 km and cover some 80 percent of the surface of Venus, has been determined by the Venera landers (*4*) and by the Pioneer Venus probes (*5*) to be 735 ± 10 K. On the basis of the global altitude measurements of the Pioneer Venus radar and the nearly adiabatic lapse rate of −9 K/km determined by the Venera and Pioneer Venus probes, Theia Mons and the equatorial highlands at a radius of about 6056 km should be 40 K colder than the median plains, an effect that would be barely discernible in Fig. 1, where the statistical measurement errors approach 15 K. How, then, can we explain the substantially cooler emission temperatures actually observed?

The thermal power emitted by an object at radio wavelengths, where the Rayleigh-Jeans approximation to the emission law is valid, depends on the product of its physical temperature (T_p) and its emissivity (e). When viewed from above, the total power seen from a planet per unit surface area will be the sum of an emitted and a reflected component and will, in general, vary with θ, the angle of incidence to the local surface normal at which the observation is made.

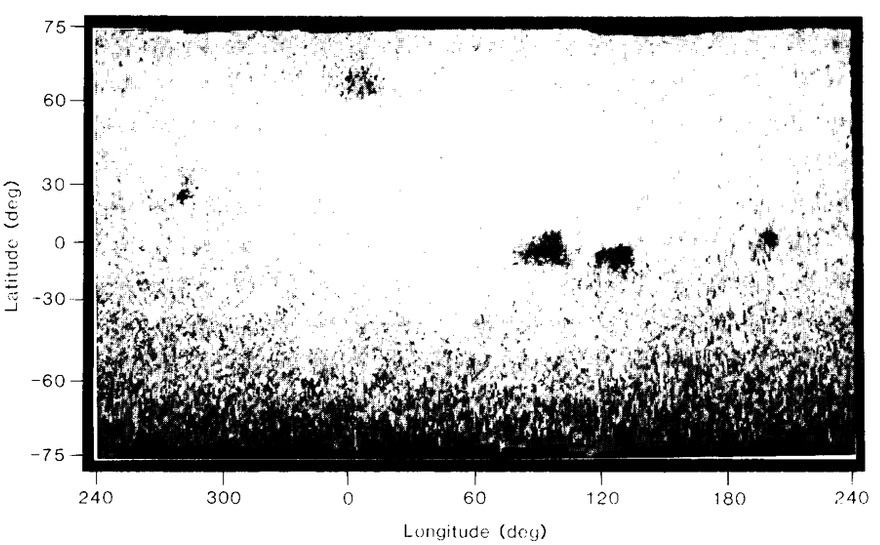

Fig. 1. Radio brightness temperatures of Venus at 17-cm wavelength as observed by the Pioneer Venus radar mapper experiment. The brightness temperature of most of the planet's surface has been taken to be 635 K; under this assumption, the darkest (coolest) areas have a brightness temperature of 405 ± 30 K.